Experimental Neurology 315 (2019) 60–71

Contents lists available at ScienceDirect

Experimental Neurology

journal homepage: www.elsevier.com/locate/yexnr

Research paper

Conditioning electrical stimulation promotes functional nerve regeneration

Jenna-Lynn Senger[a], K. Ming Chan[b], Haecy Macandili[a], Ashley W.M. Chan[a], Valerie M.K. Verge[c], Kelvin E. Jones[d], Christine A. Webber[a,*]

[a] Department of Surgery, University of Alberta, Edmonton, AB T6G 2H7, Canada
[b] Division of Physical Rehabilitation, University of Alberta, Edmonton, AB T6G 2G3, Canada
[c] Department of Anatomy and Cell Biology, Cameco MS Neuroscience Research Center, University of Saskatchewan, Saskatoon, SK S7K 0M7, Canada
[d] Department of Biomedical Engineering, University of Alberta, Edmonton, AB T6G 2H9, Canada

ARTICLE INFO

Keywords:
Conditioning electrical stimulation
Nerve regeneration
Conditioning crush lesion

ABSTRACT

Peripheral nerve regeneration following injury is often incomplete, resulting in significant personal and socio-economic costs. Although a conditioning crush lesion prior to surgical nerve transection and repair greatly promotes nerve regeneration and functional recovery, feasibility and ethical considerations have hindered its clinical applicability. In a recent proof of principle study, we demonstrated that conditioning electrical stimulation (CES) had effects on early nerve regeneration, similar to that seen in conditioning crush lesions (CCL). To convincingly determine its clinical utility, establishing the effects of CES on target reinnervation and functional outcomes is of utmost importance. In this study, we found that CES improved nerve regeneration and reinnervation well beyond that of CCL. Specifically, compared to CCL, CES resulted in greater intraepidermal skin and NMJ reinnervation, and greater physiological and functional recovery including mechanosensation, compound muscle action potential on nerve conduction studies, normalization of gait pattern, and motor performance on the horizontal ladder test. These findings have direct clinical relevance as CES could be delivered at the bedside before scheduled nerve surgery.

1. Introduction

Motor and sensory recovery following nerve injury is limited by the rate of peripheral nerve regrowth (1–3 mm/day), and the decreased potential of muscle reinnervation after prolonged atrophy. Consequently, recovery from peripheral nerve injury is often incomplete, resulting in long-term disability with profound personal and socioeconomic costs (Lundborg, 2000). To date, there remain no clinically feasible methods of accelerating the rate of nerve regeneration. In a rodent model however, a conditioning crush lesion (CCL) is well documented to significantly accelerate peripheral nerve regeneration. In this model, crushing a nerve seven days prior to a nerve injury promotes nerve regeneration up to five-fold (Richardson and Verge, 1987; Torigoe et al., 1999). There is an associated upregulation of regeneration-associated genes (RAGs), such as growth associated protein-43 (GAP-43), brain-derived neurotrophic factor (BDNF), phosphorylated cAMP response element binding protein (pCREB) and glial fibrillary acidic protein (GFAP). This shifts the neuron into a regenerative state and increases the production and transport of necessary structural proteins for axon extension resulting in greater sensorimotor regeneration and functional recovery (Bisby, 1985; Hoffman, 2010; Richardson et al., 2009; Ying et al., 2014). Unfortunately, CCL is not clinically feasible, and thus translation to the bedside is not possible.

An alternative technique for enhancing nerve regeneration and functional recovery that is currently being used clinically is postoperative electrical stimulation (PES) (Al Majed et al., 2000a; Al Majed et al., 2000b). However, unlike CCL, PES does not accelerate the rate of nerve regeneration but rather reduces the delay caused by staggered regeneration at the site of injury (Brushart et al., 2002). A seminal observation by Udina et al. (2008) determined that the same electrical stimulation parameters seven days prior to axotomy enhanced dorsal root ganglion (DRG) neurons neurite outgrowth to the same extent as CCL. Because PES has already been shown to be safe and well tolerated

Abbreviations: BDNF, brain derived neurotrophic factor; CCL, conditioning crush lesion; CES, conditioning electrical stimulation; CMAP, compound muscle action potential; GAP-43, growth associated protein 43; GFAP, glial fibrillary acidic protein; IENF, intraepidermal nerve fiber; ES, electrical stimulation; NCS, nerve conduction study; NMJ, neuromuscular junction; pCREB, phosphorylated cAMP response element binding protein; PES, postoperative electrical stimulation; RAG, regeneration associated genes

* Corresponding author at: Division of Anatomy, Department of Surgery, University of Alberta, 5-03 Medical Sciences Building, T6G 2H7 Edmonton, AB, Canada.
E-mail address: webber2@ualberta.ca (C.A. Webber).

https://doi.org/10.1016/j.expneurol.2019.02.001
Received 25 November 2018; Received in revised form 30 January 2019; Accepted 1 February 2019
Available online 05 February 2019
0014-4886/

in a number of clinical trials (Barber et al., 2018; Gordon et al., 2010; Wong et al., 2015), electrical stimulation may be an appealing strategy of delivering a CCL-like treatment to patients with peripheral nerve injury. We therefore proposed using the well-established technique of electrical stimulation in a different context, to determine if it we could non-injuriously induce a conditioning-like effect.

In a recent proof of principle study, we demonstrated that conditioning electrical stimulation (CES), delivered prior to nerve transection and microsurgical repair of the fibular (common peroneal) nerve, upregulates RAGs and accelerates peripheral nerve regeneration in a manner similar to a CCL (Senger et al., 2017). While these early findings seem promising, it remains to be determined whether these improvements in regeneration translate to enhancement in reinnervation and, of great practical relevance and clinical importance, function. Therefore, the goal of this study is to test the hypothesis that, in addition to increasing the rate of nerve regeneration, CES also enhances motor and sensory functional recovery. We found that while CES had a similar effect on accelerating nerve regeneration as CCL, it produced even greater function recovery.

2. Methods

2.1. Animals

Healthy adult male Sprague Dawley rats (200 g; Charles River laboratory) were placed under the care of Health Sciences Laboratory Animal Services at the University of Alberta. They were housed 2 animals per flat-bottomed betachip-lined cages, under 12h on/off light conditions, with *ad libitum* standard rat chow and water. All experimental procedures were approved by the University of Alberta Animal Research Ethics Board, and surgeries were performed in a dedicated animal surgical facility.

2.2. Experimental design

Animals were randomly divided into four equal cohorts determined by the type of conditioning applied to the tibial nerve: a) CES, b) CCL, c) sham electrical stimulation controls (Sham-ES), and d) unconditioned control animals. Experimental groups were as follows: 24 animals were used for tibial nerve regeneration studies (culled 14 days post-conditioning, $n = 6$/cohort), 40 animals were used for behavioral testing (culled 8 weeks post-conditioning, $n = 10$/cohort), 36 animals were used for regeneration-associated gene (RAG) analysis at the DRG (culled 3 days post-conditioning, $n = 5$/cohort for immunohistochemistry, $n = 4$/cohort for Western blot analysis); and 36 animals were used for tibial nerve regeneration studies comparing 5, 14 and 21 days regeneration ($n = 4$ animals/cohort).

2.3. Conditioning surgery

Prior to skin incision, all animals were anesthetized with inhalational isoflurane (2%, titrated at 1–2 L/min to maintain a surgical anesthetic plane), and received a single 0.01 mg/Kg dose of subcutaneous buprenorphine. Opioids were chosen rather than nonsteroidal anti-inflammatories, as inflammation has been implicated in mounting a conditioning effect (Niemi et al., 2016; Niemi et al., 2013). A longitudinal incision was made over the lateral aspect of the right hind paw to gain access to the superficial posterior compartment of the leg. The gastrocnemius muscle was elevated through blunt dissection and the tibial nerve was isolated as it emerged between the gastrocnemius head bifurcation. Nerve conditioning was performed as previously described (8): (a) CES: stainless steel wires with ends bared of insulation were connected to an SD-9 stimulator (Grass Instruments Co., Quincy, MA). The cathode wire was wrapped around the tibial nerve at the level of the gastrocnemius head bifurcation and the anode wire was placed into the belly of the tibialis anterior muscle. A continuous train of electrical stimulation (20 Hz of 0.1 ms duration balanced biphasic pulses) as previously described in PES was delivered for 1 h with voltage titrated to maintain a visible twitch in the lower limb flexors (Al Majed et al., 2000b; Geremia et al., 2007); (b) CCL: the tibial nerve was crushed at the level of the gastrocnemius muscle head bifurcation using a non-toothed fine hemostat (5 mm tip) for 10 s; (c) sham-ES: two wires were positioned using the same landmarks as CES and left in place for 1 h, but no current was delivered; d) unconditioned: no surgical intervention was performed prior to the test lesion and microsurgical repair. Animals were reassessed the day following all surgical intervention.

2.4. Nerve transection and microsurgical repair surgery (test lesion)

A nerve repair surgery was performed on all animals except those in which the DRGs were isolated for RAG expression 3 days post-conditioning. Animals recovered from conditioning for 7 days prior to tibial nerve transection and microsurgical repair. The animals were anesthetized with inhaled isoflurane and a single dose of buprenorphine (0.01 mg/Kg) provided analgesia. An incision was made posterior to the lateral middle third of the palpable femur, and the sciatic nerve was identified and isolated. The sciatic nerve was traced distally to its site of trifurcation and, 1 cm distal to this landmark, the tibial nerve was isolated and transected. Immediately following the axotomizing transection, an epineurial repair was performed using 9–0 silk suture under 3.5× loupe magnification. The hamstring muscles were re-suspended and the skin closed using 3–0 Vicryl suture (Ethicon Inc., Somerville, NJ). Animals received 0.01 mg/Kg subcutaneous buprenorphine the following day.

2.5. Tissue processing

Animals were euthanized at the appropriate time points for the outcome studied: 3 days post-conditioning (RAG analysis), 5, 14 and 21 days post-coaptation (length of regeneration studies), and 8 weeks post-nerve repair (behavioral studies). Euthanasia was accomplished by carbon dioxide inhalation followed by exsanguination by left cardiac ventricle puncture.

The tibial nerve was re-exposed and the site of the microsurgical repair identified. The nerve was carefully dissected from the fibular and sural nerve branches as well as from surrounding scar and soft tissues. Once harvested, the nerve was placed on a 3 cm segment of toothpick to stabilize the proximal stump, regenerating tip, and distal stump. The proximal sciatic nerve was then traced back to its vertebral column origins for accurate identification and extraction of the L4 and L5 DRGs. Tissues were fixed in Zamboni's fixative (paraformaldehyde, picric acid, NaOH, American MasterTech Scientific, Lodi, CA) for 4 h, rinsed with 0.01 M phosphate buffered saline (PBS) (Thermo Fisher Scientific, Waltham, MA) five times, post-fixed in 30% sucrose solution (Thermo Fisher Scientific, Waltham, MA) overnight at 4 °C, then frozen in Optimum Cutting Temperature (OCT) (Sakura Finetek, Torrance, CA) using indirect exposure to liquid nitrogen. Both the nerve and DRGs were cut into 12 µm sections (nerve was cut longitudinally) and thaw-mounted on Superfrost Plus microscope slides (Thermo Fisher Scientific, Waltham, MA). Slides were stored at –80 °C until processing.

The gastrocnemius muscles were harvested from the bilateral lower limbs, from the insertion point of the Achilles tendon onto the calcaneus to the attachment points of the two muscle heads on the proximal tibia. The ipsilateral muscle was represented as the percentage weight of the uninjured contralateral control limb. To prepare for NMJ immunocytochemistry, the muscle from the injured limb was fixed in Zamboni's solution overnight, rinsed five times with PBS, sunk in 30% sucrose overnight (4 °C), then flash-frozen using liquid nitrogen in OCT. Sections of 20 µm were cut in the cryostat and stored at –80 °C.

Footpads of the injured limb were collected at 8 weeks post-nerve repair. A 3 mm biopsy punch (Acuderm Inc., Fort Lauderdale, FL) was used to collect tissue from plantar footpad which was fixed in 2%

paraformaldehyde, lysine, periodate (PLP) fixative for 16–20 h at 4 °C, rinsed 5× in Sorensen's phosphate buffer, then cryoprotected overnight at 4 °C in 20% glycerol (Thermo Fisher Scientific, Waltham, MA)/0.1 M Sorensen's phosphate buffer. Tissue was frozen in OCT and cut into 20 μm sections on Superfrost-Plus microscope slides. Slides were stored at -80 °C until processing.

2.6. Behavioral and physiological outcomes

Animal behaviour testing was performed at 6.5, 7, 7.5 and 8 weeks following nerve repair. All tests were performed by the same examiner who was blinded to the conditioning of the animals. Sensory re-innervation was analyzed using von Frey filaments. Motor testing included gait analysis for toe spread, horizontal ladder task for motor dexterity, and nerve conduction studies for compound muscle action potentials (CMAPs).

Sensory testing was performed using von Frey filaments at all four time-points post-nerve repair. Animals received 30 min of acclimatization after being placed in a plexiglass cage with wire mesh flooring. Increasing force was placed on the plantar aspect of the animal's injured foot within the distribution of the tibial dermatome, using calibrated von Frey monofilaments (1.4–15 g). Each paw was probed five times with each monofilament for a 3 s duration with enough force to cause bending of the monofilament. A positive result was recorded when the animal withdrew his paw for three consecutive probes of an individual monofilament.

Gait analysis was performed at 7 and 8 weeks to analyze the function of the intrinsic foot muscles innervated by the tibial nerve. The animals were placed in a specially-designed transparent narrow walkway measuring 48 cm in length, designed with an adjustable mirror underneath that allows for simultaneous visualization of the lateral view of the animal and its plantar paw. A ruler projected in the mirror from the walking path served as reference. Video was taken of the animals walking the length of the track three times per testing session. The video was then analyzed and individual screenshots were taken of each footstep when the animal was weight-bearing on that limb. Only images where the position of all toes could be adequately visualized were analyzed. A minimum of 10 images per foot were analyzed per testing session. The distance between the first and last toe was measured on the injured right, and control left sides. Toe spread of the injured side was reported as a percentage of the uninjured contralateral control.

The horizontal ladder task was performed a total of four times, at 6.5, 7, 7.5, and 8 weeks post-nerve repair. The horizontal ladder itself consisted of an elevated (48 cm) horizontal ladder composed of clear plexiglass. At each test session, the animal was evaluated on three separate attempts at crossing the ladder. Placement of ladder rungs was changed between each testing session to prevent the rats from learning the course. Videos taken of the animals crossing the horizontal ladder were analyzed in a blinded fashion on a frame-by-frame basis. Each placement of the foot on a ladder rung was graded on a scale of 0–6 based on the scoring system developed by Metz and Whishaw (Metz and Whishaw, 2009): a total miss (score 0), deep slip (score 1), slight slip (score 2), replacement (score 3), correction (score 4), partial placement (score 5) or correct placement (score 6). The average score of the injured limb was calculated for each attempt on the ladder.

Nerve conduction studies (NCS) were performed on both lower limbs at 8 weeks post-nerve repair. Animals were anesthetized using inhaled isoflurane. Supramaximal electrical stimulation was performed at the knee and the recording leads were placed in the plantar footpad to record from the intrinsic foot muscles. The location of the lead was adjusted to detect the CMAP with the maximum amplitude and sharpest rise time. This was used to quantify the extent of successful muscle reinnervation in the foot.

2.7. Immunofluorescence

Slides were warmed to room temperature prior to antigen retrieval in a 60 °C citrate buffer (10 mM sodium citrate, 0.05% Tween-20, pH 6.0; Thermo Fisher Scientific, Waltham, MA) for 20 min and then they were cooled to room temperature. After washing the slides three times in 0.01 M PBS for 5 min, slides were permeabilized with 0.1% Triton-100× (Thermo Fisher Scientific, Waltham, MA) for 10 min. Individual sections were blocked in 10% normal goat serum (MP Biomedicals, Santa Ana, CA) and 3% bovine serum albumin (BSA) (Sigma-Aldrich, St Louis, MO) in 0.01 M PBS for 90 min. Primary antibodies were diluted in a solution of 0.01 M PBS containing 3% BSA, and applied to tissue sections overnight at 4 °C. DRG sections were stained with the primary antibodies: rabbit anti-GAP-43 (1:400, Millipore), rabbit-anti-GFAP (1:500, DAKO, Santa Clara, CA), chicken anti-BDNF (1:500, Promega, Madison WI), and rabbit anti-phosphorylated CREB (1:500, Cell Signaling Technology, Danvers, MA). Nerve sections were stained with 1:500 mouse anti-neurofilament-200 (NF200) (Sigma-Aldrich, St Louis, MO). Muscle sections were first labeled with 1:500 mouse anti-NF200 to stain the innervating nerve and then stained with (1:1000 dilution) conjugated anti-α-bungarotoxin for 20 min. Footpad intraepidermal nerve fibers were labeled with 1:1000 rabbit anti-protein gene product 9.5 (PGP9.5) (Encor Biotechnology Inc., Gainesville, FL). The next day, slides were washed three times for 5 min each with 0.01 M PBS, and the secondary antibodies, diluted in a solution of 0.01 M PBS containing 3% BSA, was applied for 90 min at room temperature. Secondary antibodies included Cy3-conjugated goat anti-mouse (Sigma-Aldrich), Alexa Fluor 488-conjugated goat anti-rabbit IgG (Invitrogen, Carlsbad, CA), and donkey-anti-chicken 594 (Thermo Fisher Scientific). DRG slides were counterstained with nuclear stain NucBlue (Thermo Fisher Scientific). All slides were then mounted with a coverslip using 50% glycerol in 0.01 M PBS. The specificity of secondary antibodies was employed by experiments in which the primary antibody was omitted, revealing the absence of nonspecific staining.

All slides were qualitatively assessed to ensure there was no discernable slide-to-slide variation for the same marker within individual treatment groups. Quantitative analysis was performed in a blinded manner on DRG sections to identify alterations in immunofluorescence signal. To ensure reliability in the comparison between experimental groups, all sections for each antibody were processed for immunofluorescence in an identical, parallel manner. Digital images were taken under identical fluorescence exposures using the 20× objective lens of a Zeiss Axio Imager fluorescence microscope. Twelve representative DRG sections were analyzed for each animal ($n = 5$ animals/cohort). The intensity of the immunofluorescence was quantified by identifying neurons with NucBlue-stained nuclei and manually circling the perimeter of each individual DRG neuron using ImageJ software (ImageJ; Rasband WS). Cells were deemed positive for GAP-43 or BDNF expression as determined by the level of immunofluorescence of neurons considered to be devoid of positive signal upon scrutiny at higher magnification. Data was further subdivided into 'low to moderately' GAP-43 or BDNF immunopositive and 'highly' immunopositive based on natural breaks identified on analysis of scatterplots (data not shown) representing the different animals and treatment groups. Expression of pCREB and GFAP was analyzed using binary evaluation; DRG neurons were classified as "positive" or "negative" based on the presence or absence of positive staining in the nuclei or satellite glial cells (SGCs), respectively.

Nerve tissues were cut longitudinally (12 μm) to preserve the proximal stump coapted to the distal stump. Sections were processed for immunohistochemistry against neurofilament-200 (NF-200) to label individual axons. Under fluorescent microscopy, the unique morphological patterns were identified to differentiate the regenerating axons from the degenerating ones. The length of axonal extension and the number of regenerating axons were measured (250 μm intervals) from

the site of repair to the most distal point of regeneration containing a minimum of 10 axons.

Muscle sections were evaluated with confocal microscopy to identify innervated neuromuscular junctions (NMJs) determined by NF200, to identify the innervating axon, and α-bungarotoxin, to label the acetylcholine receptors. The mean innervated number of NMJs of each cohort was quantified by averaging the total number of NMJs in 6 separate tissue sections per animal.

Footpad sections were imaged at 40× magnification capturing 5–6 adjacent fields for a total of 10–15 fields per animal. A z-stack of 1 μm steps was imaged for each field, and using ImageJ software, the intraepidermal nerve fiber (IENF) density was determined by counting the number of positively stained axons (PGP9.5) crossing the dermal-epidermal junction (number of IENF/mm).

2.8. Western blot analysis

Cellular protein was isolated from DRGs collected 3 days following conditioning by homogenizing samples with RIPA buffer and protease inhibitor. Protein concentrations were determined with a BCA Protein Assay Kit (Pierce) and 25 μg of solution (protein, β-mercaptoethanol, RIPA buffer and protease inhibitor) was loaded into each well of precast gel cassettes (Mini-Protean TGX Stain-Free Protein Gel, 4–20%). Proteins were transferred overnight onto PVDF membrane (Millipore) and bands were imaged for total protein. The membrane was placed in blocking solution (5% BSA in Tris-buffered saline) for 1 h, then overnight in the primary antibodies rabbit anti-GAP43 (1:1000) or rabbit anti-BDNF (1:1000), in a solution of 2.5% BSA in Tris-buffered Saline. Following secondary antibody (Goat anti-rabbit IgG HRP, 1:20,000), the blot was exposed to enhanced chemiluminescent (ECL; Lumi-Light Plus, Roche Diagnostics) for signal detection and band images were captured. Antibody expression was normalized to total protein.

2.9. Statistical analyses

Results are presented as the mean ± standard error mean (s.e.m). Differences in individual animals of each cohort were analyzed using a one-way analysis of variance (ANOVA) followed by Bonferroni *post hoc* test to compare means between groups. A two-way ANOVA was performed to compare sensory and motor behavioral performance between cohorts. In cases where a significant interaction between the factors: time and treatment allocations was found, *post hoc* analysis using Tukey test was done. Statistical significance was accepted with a level of $p < 0.05$. All statistical analyses were performed using STATA 14 (StataCorp LP, Collagen Station, Texas).

3. Results

3.1. CES and CCL of the tibial nerve enhances the length and magnitude of axonal regeneration

The regenerative potential of CES, CCL, sham-ES, and unconditioned animals were compared ($n = 6$ animals/cohort). One week following conditioning, the tibial nerve was re-exposed and a complete nerve axotomy was performed 10 mm proximal to the previous conditioning site. The proximal and distal stumps were immediately repaired with two epineurial stitches; this coaptation was performed to guide regenerating nerve fibers and to mimic the clinical treatment for complete peripheral nerve injuries. One week following nerve transection and repair (14 days after conditioning), animals were euthanized and the tibial nerves were harvested and processed for neurofilament (NF200) immunofluorescence to measure the extent of nerve regeneration (Fig. 1). Both CES and CCL significantly improved the lengths of axon regeneration by 2.3–2.5 fold compared to the sham-ES and unconditioned animals. The length of axonal extension for CES animals (6.35 ± 1.0 mm) was similar to CCL (6.73 ± 1.0 mm), and significantly longer than sham-ES (2.67 ± 0.5 mm) or unconditioned (2.78 ± 0.9 mm) control nerves. This difference was highly significant for all length comparisons of CES and CCL to sham-ES or unconditioned control animals ($p < 0.001$) (Fig. 1E, x-axis). There was no difference between the CES and CCL groups ($p = 0.287$). Similarly, both CES and CCL had an increased number of total regenerating nerve fibers compared to the unconditioned control cohorts (Fig. 1E, y-axis, $p < 0.001$ for all). At the cut site (Fig. 1A-D, dashed lines), the number of regenerating fibers entering the distal nerve stump was 132 ± 9 axons in CES and 113 ± 10 axons in CCL whereas a significantly lower number of axons entered the regeneration site in the sham-ES (62 ± 9 axons) or unconditioned animals (68 ± 5 axons) ($p < 0.001$ for all). There were significantly greater numbers of CES and CCL regenerating axons identified over the entire length of regeneration compared to the control nerves ($p < 0.001$ for all).

3.2. CES of the tibial nerve improves sensory innervation greater than CCL

Forty animals ($n = 10$/cohort) were examined between 6.5 and 8 weeks after cut and microsurgical repair to compare functional outcomes with or without conditioning (Fig. 2A). At 6.5 weeks of regeneration, von Frey filament tests revealed that CES animals responded to 8.5 ± 1.0 g whereas both sham-ES and unconditioned animals were unresponsive to all filament weights ($p < 0.001$); CCL animals required 16.5 ± 3.4 g of mechanical stimulation to elucidate a positive response ($p = 0.06$ compared to CES). At 7 weeks, the average weight required to evoke three consecutive positive responses in the CES animals was 8.5 ± 1.0 g, which showed a trend of increased responsiveness compared to CCL (9.8 ± 1.8 g, $p = 0.077$), sham-ES (10.3 ± 1.9 g, $p = 0.054$) or unconditioned animals (13.8 ± 1.3 g, $p < 0.01$). By 7.5 weeks, animals in the CES cohort had significant sensory improvements, with responsiveness to 4.5 ± 0.5 g, which was significantly less than in CCL (6.5 ± 0.5 g, $p < 0.05$), sham-ES (9.3 ± 0.7 g, $p < 0.01$) or unconditioned animals (15.3 ± 3.8 g, $p < 0.001$) (Fig. 2B). Similarly, at 8 weeks, CES animals continued to improve, requiring an average of only 3.0 ± 0.6 g, significantly less than that required by animals in the CCL (6.5 ± 1.0 g, $p < 0.05$), sham-ES (9.3 ± 0.7 g, $p < 0.001$) or unconditioned cohorts (10.8 ± 1.5 g, $p < 0.001$). Two way ANOVA of weeks 7 and 8 revealed a significant interaction between time and treatment groups ($p < 0.05$). *Post hoc* analysis revealed that the CES group performed significantly better compared to the other groups ($p < 0.05$). These data strongly suggest increased sensitivity of the CES animals compared to all other cohorts. These behavioral differences are corroborated by evidence from microscopic evaluation of injured footpads confirming greater epidermal reinnervation in CES animals. At 8 weeks, CES animals had a greater number of sensory intraepidermal nerve fibers (IENFs) crossing the dermal-epidermal junction (25.5 ± 1.6 axons/μm) compared to CCL (19.3 ± 1.3 axons/μm, $p < 0.01$), sham-ES (7.5 ± 1.1 axons/μm, $p < 0.001$) or unconditioned controls (8.9 ± 1.9 axons/μm, $p < 0.001$) (Fig. 2C-G).

3.3. CES of the tibial nerve improves motor outcomes greater than CCL

Increased sensory reinnervation was accompanied by improved functional outcomes. Gait analysis at 7- and 8 weeks post-nerve repair revealed that CES significantly improved reinnervation of the foot interosseous muscles which are responsible for toe spread (Fig. 3A). At 7 weeks post-nerve repair, the average toe spread of the injured paw among CES animals was 55.2 ± 1.6% of their uninjured paw, which was greater than the recovered toe spread in the CCL group at 45.7 ± 4.2%; this trend however failed to show significance ($p = 0.08$). CES had significantly greater toe spread recovery compared with sham-ES (29.5 ± 0.4%; $p < 0.001$) or unconditioned animals (40.1 ± 1.8%; $p < 0.001$). However, by 8 weeks post-nerve repair, toe spread recovery was significantly greater in the CES (58.3 ± 1.6%)

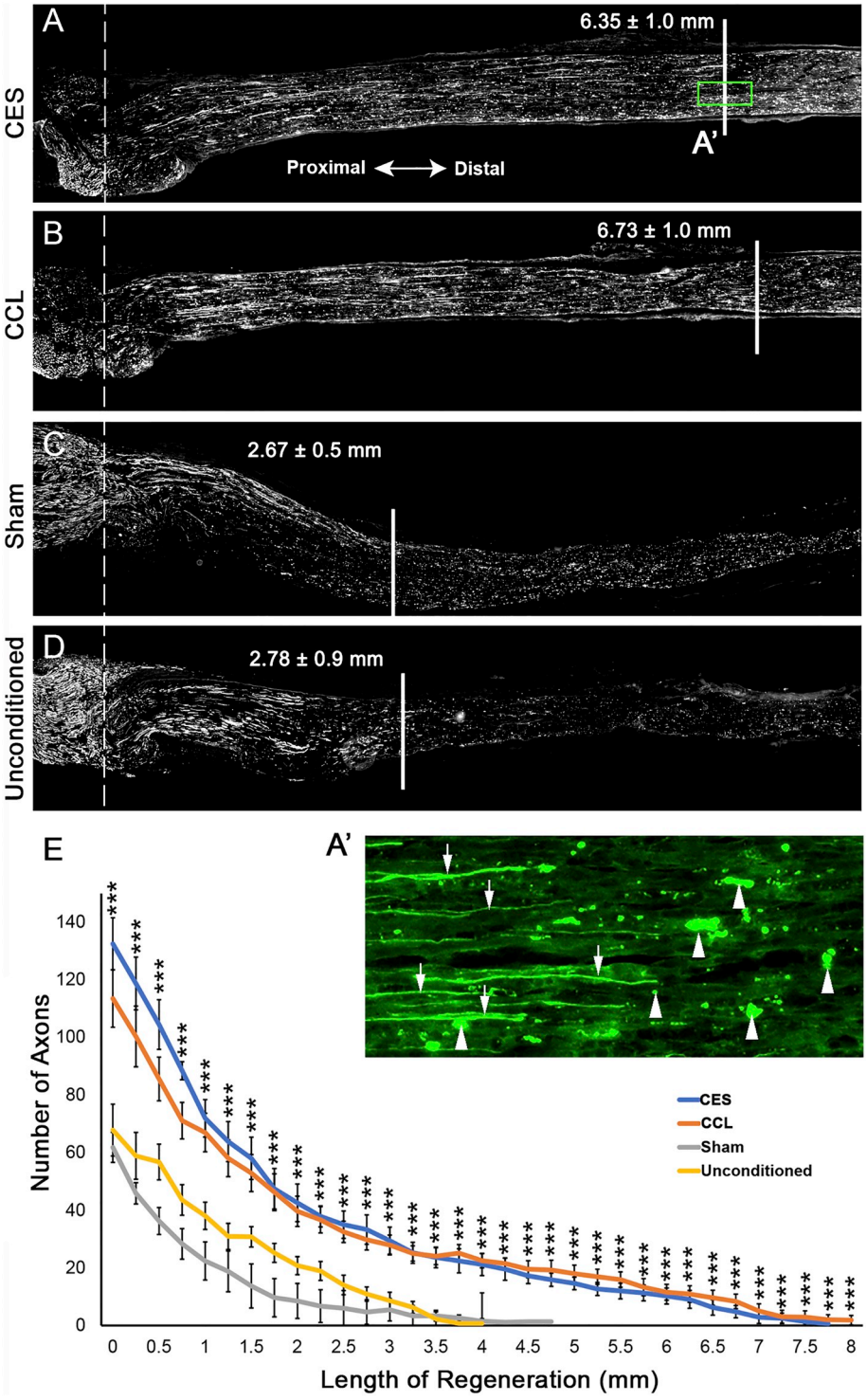

Fig. 1. CES promotes nerve regeneration as efficiently as CCL. Representative photomicrographs of NF200 labeled longitudinal tibial nerve sections at the regeneration site on day 14. These nerves were conditioned by CES (A), CCL (B), sham-ES (C) or no conditioning (D) on day 0 and then transected and repaired on day 7. Regenerating axons were identified based on their linear morphology which is distinct from the punctate appearance of NF200-positive degenerating axons. Dashed white lines depict the site of cut and coaptation and the solid vertical white lines indicate the distal-most point of regeneration (defined as the distal-most site where a minimum of 10 axons were counted). Green inset (A') depicts a magnified view of the axons at the distal tip of regeneration (arrows) with staining distal to this point being NF200-positive axons undergoing Wallerian degeneration (arrowheads). Line graph (E) depicts the average length of axonal regeneration (x-axis) and the number of regenerating axons (y-axis). Axons conditioned with CES (blue line) or CCL (orange line) had a similar number of axons present at each 250 μm interval distal to the injury site which was considerably more than sham-ES (grey line) or the unconditioned cohorts (yellow line). At all sites in which axon length and number were measured, the CES and CCL animals were significantly higher than the sham or unconditioned controls (***$p < 0.001$, $n = 6$ animals/cohort).

compared with the CCL group (48.1 ± 7.9%; $p < 0.01$) (Fig. 3B, C). Toe spread recovery of the sham-ES and unconditioned controls remained largely unchanged from the week prior, at 28.8 ± 1.1% ($p < 0.001$) and 39.3 ± 7.4% respectively ($p < 0.01$). Regression analysis and two way ANOVA of weeks 7 and 8 revealed a significant interaction between time and treatment groups ($p < 0.05$, Fig. 3A). Post-hoc analysis revealed that in the CES group, the restoration of toe spread distance was significantly better than the other groups. These data strongly suggest greater reinnervation to the intrinsic foot muscles in the CES animals and therefore wider toe spread compared to all other cohorts.

Horizontal ladder performance was improved in CES animals compared to all other cohorts (Fig. 3D). At 6.5 and 7 weeks, the average paw placement score for the injured limb was 5.3 ± 0.1 out of a maximum possible score of 6 in the CES animals while the average score for CCL animals was 4.9 ± 0.3 ($p = 0.218$). CES animals had a higher foot placement score compared to sham-ES (4.5 ± 0.3; $p < 0.05$) and unconditioned animals (3.8 ± 0.2; $p < 0.001$). At 7.5 weeks post-nerve repair, a significantly greater foot placement score was observed in CES animals (5.5 ± 0.1) as compared to CCL (5.2 ± 0.1; $p < 0.05$), sham-ES (4.08 ± 0.1; $p < 0.001$) or unconditioned controls (4.0 ± 0.1; $p < 0.001$) (Fig. 3E). At 8 weeks

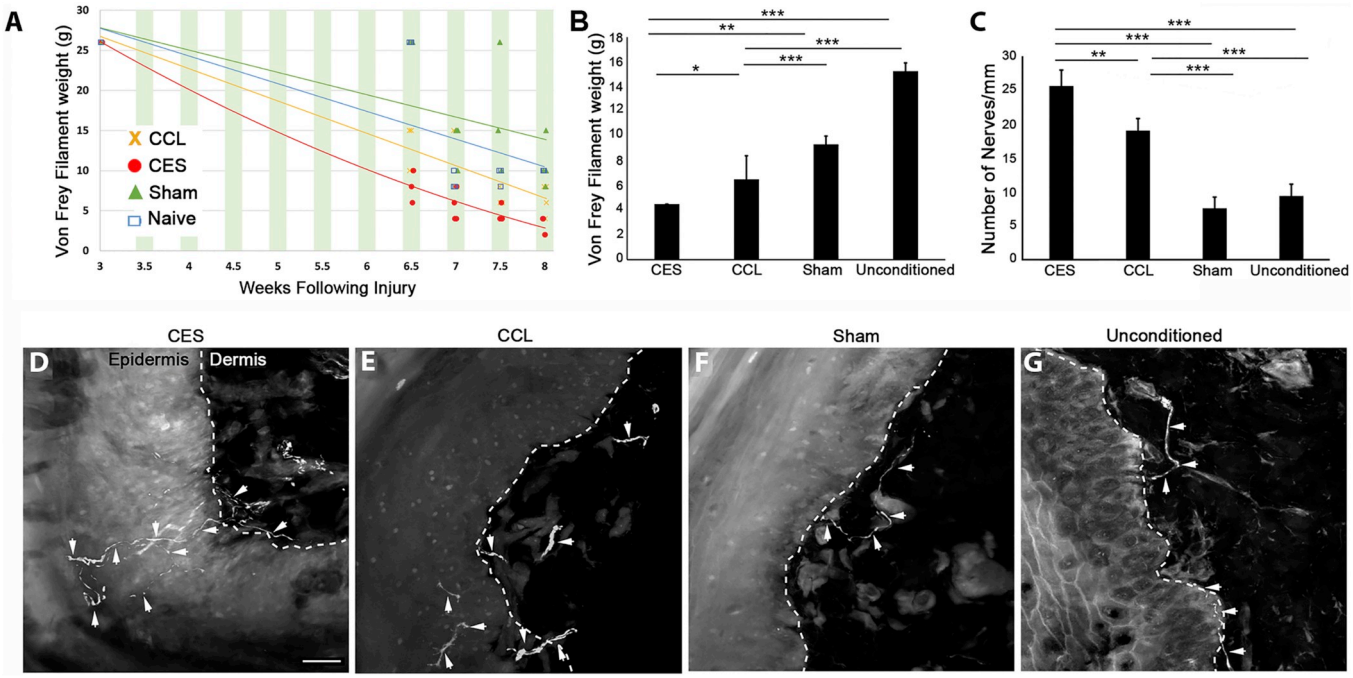

Fig. 2. CES promotes significantly greater sensory reinnervation than to CCL. (A) Regression analysis of von Frey tests at 6.5–8 weeks demonstrates greater sensory recovery in CES animals compared to CCL, sham-ES, and unconditioned controls. Two-way ANOVA comparing filament weight and time at weeks 7 and 8 confirm significantly improved reinnervation in the CES cohort compared to CCL ($p < 0.05$). (B) Representative histogram of a single time point demonstrates that 7.5 weeks after cut and coaptation, CES conditioned tibial nerves had significantly greater sensory recovery compared to CCL (*$p < 0.05$), sham-ES (**$p < 0.01$) and unconditioned (***$p < 0.001$) animals (One-way ANOVA). (C-G) At 8 weeks post-nerve transection and repair, skin biopsies were harvested from the plantar footpads of each animal and tissues (12 μm sections) were processed for intraepidermal nerve fiber innervation. (D-G) *Z*-stacks (1 μm) were imaged with confocal microscopy and the total number of PGP9.5 label axons (arrowheads) were counted as they crossed the dermal-epidermal junctions (dashed lines) of CES (D), CCL (E), sham-ES (F) and unconditioned (G) samples. (C) Quantification revealed there was significantly more nerve reinnervation per μm of epidermis in CES compared to CCL (**$p < 0.01$), sham-ES (***$p < 0.001$) and unconditioned (***$p < 0.001$) footpads (One-way ANOVA). Scale bar is 25 μm; $n = 10$ animals/cohort for all sensory tests.

post-nerve repair, CES animals again performed superiorly (5.4 ± 0.1) to the CCL (4.7 ± 0.1; $p < .005$), sham-ES (4.2 ± 0.1; $p < 0.001$) or unconditioned (3.5 ± 0.4; $p < 0.01$) cohorts. Two-way ANOVA of weeks 7 and 8 regression analysis revealed a significant interaction between time and treatment allocations ($p < 0.05$, Fig. 3D). Post-hoc analysis revealed that animals in the CES group performed significantly better than those in the other groups. These data indicate that at 8 weeks, the CES animals have improved foot placement scores compared to CCL and the two control cohorts.

As a final measure of functional improvement, nerve conduction studies were performed at 8 weeks post-nerve repair. Animals that had previously been conditioned with electrical stimulation had greater CMAP amplitudes compared to those that did not receive conditioning or CCL (Fig. 3F). The average CMAP amplitude for the injured limb of the CES animals was 45.7 ± 12.7% that of the uninjured leg. This was significantly higher than that recorded from the CCL group (12.9 ± 4.0%; $p < 0.05$), sham-ES (4.7 ± 0.9%; $p < 0.05$) or unconditioned control (6.0 ± 1.2%; $p < 0.05$) cohorts.

Functional studies were confirmed by tissue analysis. Gastrocnemius muscles were harvested from both the injured and contralateral limbs (Fig. 4A-D) in all experimental groups and examined for evidence of reinnervation indirectly by muscle mass (4E) and directly by assessment of reinnervated NMJs (4F-J). Animals conditioned with CES had restored significantly more muscle mass in the gastrocnemius muscle compared to all other cohorts (Fig. 4E). The average percentage of muscle mass (normalized to contralateral limb) in the CES cohort was 64.4 ± 4.3%, which was significantly greater than the CCL (54.2 ± 1.9%, $p < 0.05$), sham-ES (49.4 ± 2.0%, $p < 0.01$), or unconditioned control groups (41.2 ± 3.6%, $p < 0.01$). Increased muscle mass of CES following nerve transection and repair suggests reinnervation, which rescues muscle atrophy. Reinnervation of the gastrocnemius muscle was confirmed by quantifying reinnervated NMJs (Fig. 4F-J). Gastrocnemius muscle (50 mm^2 per tissue section) from each animal was stained with α-bungarotoxin to label the acetylcholine receptors, and NF200 to identify the innervating motor axons (together representing innervated NMJs as shown in Fig. 4G'). Significantly more innervated NMJs were identified in CES (19.1 ± 0.2) compared to CCL (13.4 ± 1.3, $p < 0.05$), sham-ES (4.5 ± 0.4, $p < 0.001$) or unconditioned animals (4.0 ± 0.1, $p < 0.001$) (Fig. 4J).

3.4. Tibial nerve CES and CCL similarly upregulate expression of regeneration-associated genes (RAGs)

As CES consistently demonstrated superior behavioral and functional outcomes at 2 months of regeneration compared to CCL, we hypothesized the two conditioning paradigms may have different effects on the regenerative potential of sensory neurons. One explanation for the improved regeneration of CES beyond that of CCL is an increased expression of RAGs in the CES DRGs, measured by immunohistochemistry and Western blot analysis. At 3 days post-conditioning, DRGs were harvested to assess the neuronal cell body response, specifically the upregulation of GAP-43, BDNF and pCREB as well as activation of GFAP in their surrounding satellite glial cells.

Immunofluorescent labeling revealed CES and CCL similarly increased GAP-43 expression compared to controls as illustrated in the representative DRG sections (Fig. 5A). CES and CCL had a significantly increased percentage of DRG neurons expressing moderate and high levels of GAP-43 compared to controls (Fig. 5B). GAP-43 protein expression was observed in 86.8 ± 0.4% of DRG neurons conditioned

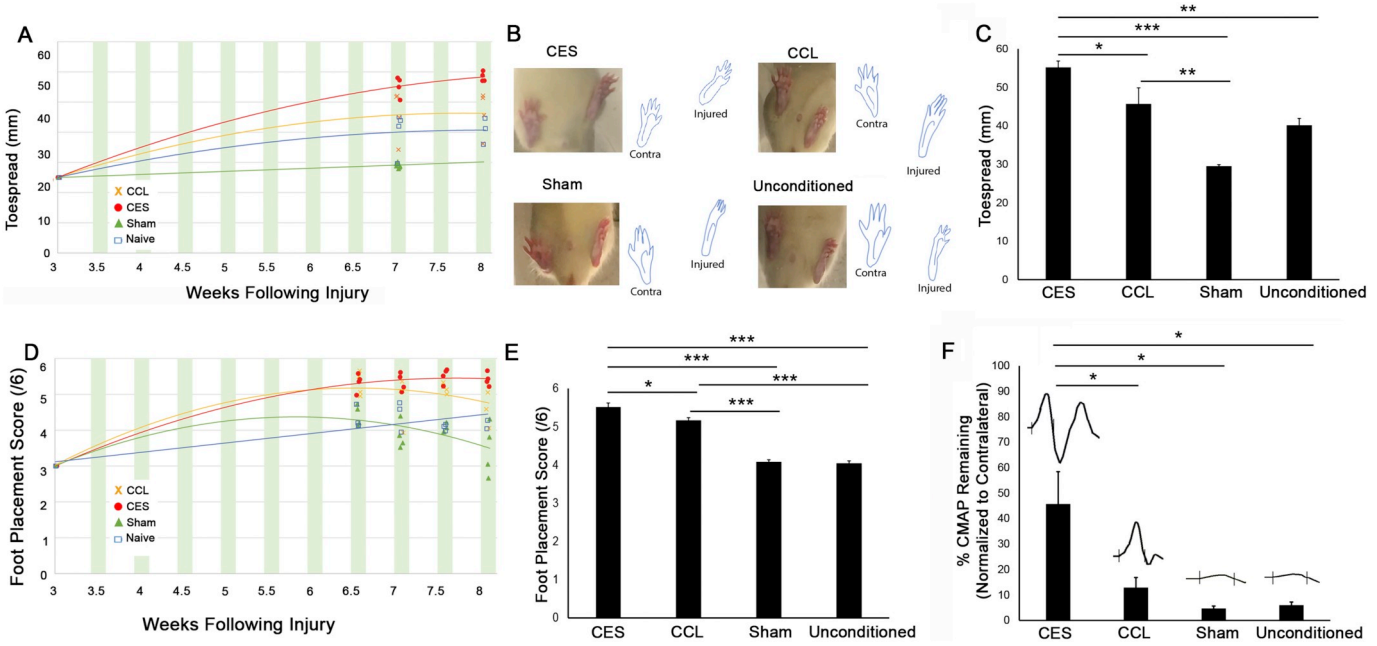

Fig. 3. CES improves functional recovery to a greater extent than CCL. Functional recovery was assessed 6.5, 7, 7.5 and 8 weeks following tibial nerve cut and coaptation in animals conditioned by CES, CCL, sham-ES, or no conditioning ($n = 10$/cohort). Toe-spread measurement between the first and fifth digit of the left (injured) foot was normalized to the contralateral control foot. (A) Regression analysis at 7 and 8 weeks revealed CES had significantly wider toe spread compared to all other cohorts ($p < 0.05$; Two-way ANOVA). (B) Representative photographs and camera lucida tracing of CES, CCL, sham-ES, and unconditioned feet are shown. (C) Representative histogram of a single time point revealed that at 7 weeks CES animals had greater toe-spread compared to CCL (*$p < 0.05$), sham-ES (***$p < 0.001$) and unconditioned (**$p < 0.01$) animals (One-way ANOVA). (D-E) The horizontal ladder task was performed to determine the number of correct foot placements and foot slips from the injured limb. (D) Regression analysis from horizontal ladder testing at 6.5, 7, 7.5 and 8 weeks is shown. Statistical analysis confirmed that at 7 and 8 weeks, CES animals had improved foot placement compared to all other cohorts ($p < 0.05$; Two-way ANOVA) revealed greater. (E) Representative histogram of a single time point revealed that at 7 weeks, CES had greater success at this motor task compared to CCL (*$p < 0.05$), sham-ES (***$p < 0.001$) and unconditioned (***$p < 0.001$) control animals (One-way ANOVA). (F) Compound muscle action potentials (CMAPs) were recorded at 8 weeks and ipsilateral muscles were normalized to the contralateral control. CES had increased CMAP amplitude compared to CCL, sham-ES, and unconditioned animals (*$p < 0.05$; One-way ANOVA).

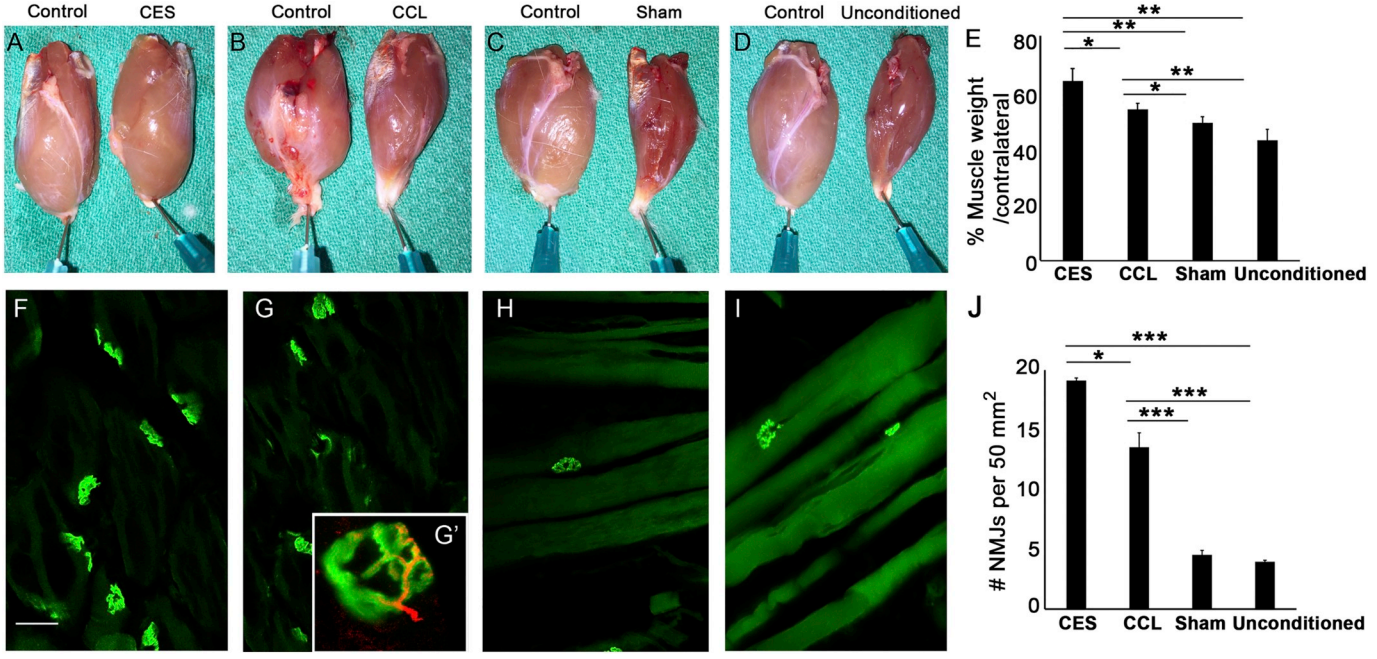

Fig. 4. CES promotes muscle reinnervation to a greater extent than CCL. (A-D) Eight weeks post-nerve transection and repair, the gastrocnemius muscles from both the injured and uninjured limbs were weighed. (E) When normalized to their contralateral controls, it was determined that the weight of the ipsilateral muscle from the CES nerves (A) had significant muscle mass recovery compared to CCL (B, *$p < 0.05$), sham-ES (C, **$p < 0.01$) and unconditioned (D, **$p < 0.01$) animals ($n = 10$ animals/cohort). (F-I) Alpha-bungarotoxin immunocytochemistry of the ipsilateral gastrocnemius muscles were processed to identify the acetylcholine receptors at the NMJs. (J) Quantification revealed CES muscle fibers (F) had significantly more acetylcholine receptors than CCL (G, *$p < 0.05$), sham-ES (H, **$p < 0.001$) and unconditioned (I, ***$p < 0.001$) muscles. All NMJs were confirmed to be innervated by NF200 (red, represented in G'). Scale bar in F is 20 μm.

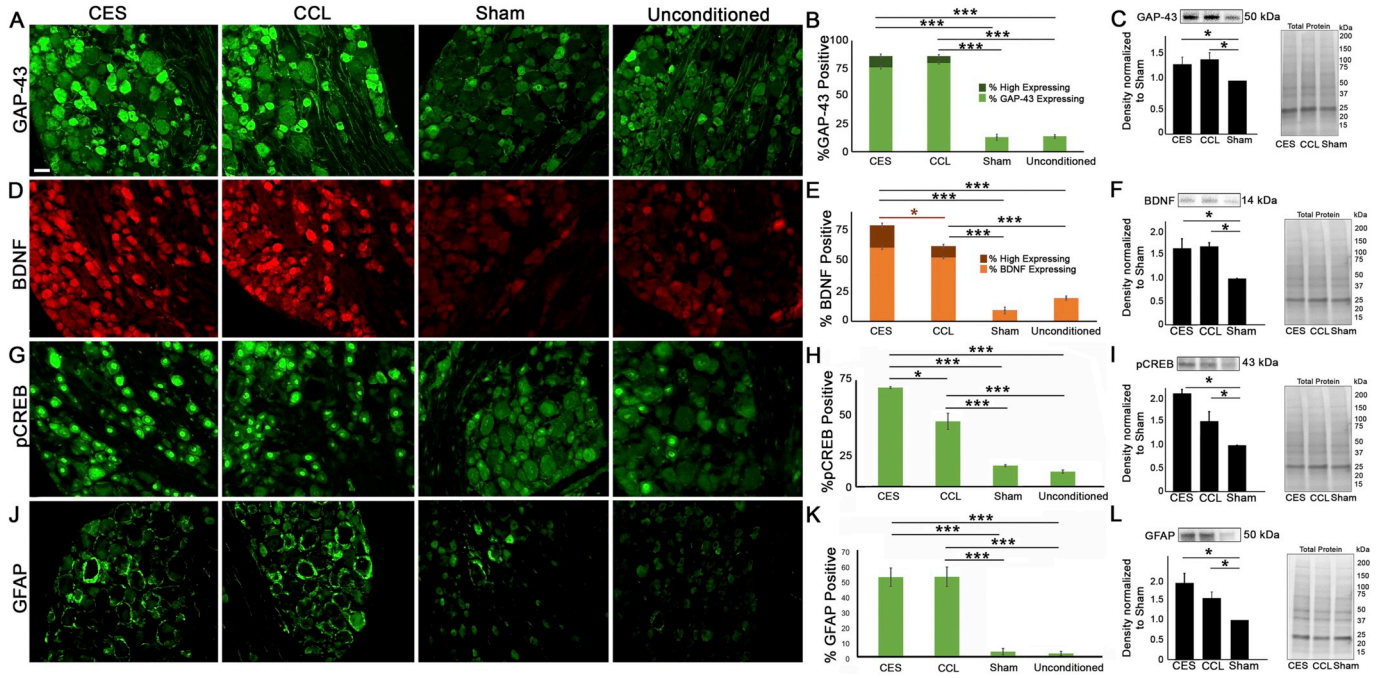

Fig. 5. CES and CCL upregulate similar levels of RAG expression. Representative photomicrographs of L5 DRG sections processed for immunofluorescence to detect GAP-43 (A) and BDNF (D), pCREB (G) and GFAP (J) expression 3 days following CES, CCL, sham-ES, or no conditioning. Elevated neuronal GAP-43 (A) and BDNF (D) expression is apparent in all sizes of DRG neurons from the two conditioned groups. Bar graph (B) depicts the mean percentage of neurons with low to moderate (light green) and high (dark green) levels of GAP-43 immunofluorescence per cohort; bar graph (E) depicts the mean percentage of neurons with low to moderate (light orange) and high (dark orange) levels of BDNF immunofluorescence per cohort. Statistical analysis compares the incidence of GAP-43 and BDNF expressing neurons in each cohort (***$p < 0.001$). (G) CES significantly increased the level of pCREB in DRG neurons compared to CCL, sham-ES, and no conditioning. (H) Bar graphs demonstrates the average pCREB immunofluorescence of 5 animals per experimental group. Statistical analysis compares the percentage of pCREB DRG neurons in each cohort (*$p < 0.05$, ***$p < 0.001$). (J) Elevated GFAP expression is apparent in SGCs from the two conditioned groups. (K) Bar graph reports the average percentage of DRG neurons surrounded by GFAP-expressing SGC cells from 5 animals per experimental group. Statistical analysis compares the percentage of DRG cell bodies surrounded by GFAP-expressing SGCs in each cohort (***$p < 0.001$). Western blot analysis confirmed significant upregulation of (C) GAP-43, (F) BDNF, (I) pCREB, and (L) GFAP protein in CES and CCL cohorts when normalized to the amount of total protein in each lane (*$p < 0.05$ for all). Scale bar represents 50 μm.

with CES, and 86.0 ± 1.5% of DRG neurons conditioned with CCL; among these positive neurons, 75.9 ± 1.5% and 79.8 ± 1.7% of DRG neurons had low to moderate immunofluorescence and 10.9 ± 1.8% and 6.2 ± 2.4% of DRG neurons had high levels, respectively. This was significantly higher than the sham-ES or unconditioned control cohorts, in which GAP-43 was detected in only 13.1 ± 2.7% and 13.7 ± 1.7% of DRG neurons, respectively, with only 0.08 ± 0.08% and 0.04 ± 0.03% of these neurons showing high levels of GAP-43 immunofluorescence ($p < 0.001$ for all). Western blot analysis confirmed similarly increased expression of GAP-43 protein in CES and CCL compared to negative controls ($p < 0.05$) (Fig. 5C).

BDNF protein expression was similarly increased in the corresponding DRGs whose tibial nerves were subjected to CES and CCL. Representative DRG sections with corresponding analysis of neuronal BDNF immunofluorescence signal demonstrated that the percentage of DRG neurons expressing BDNF compared to sham-ES and unconditioned control cohorts (Fig. 5D-E). CES and CCL upregulated BDNF expression such that 78.9 ± 3.1% and 61.8 ± 5.3% of DRG neurons had detectable levels of expression as compared to the relatively low percentages of BDNF positive neurons in sham-ES (9.2 ± 2.9%) or unconditioned (19.1 ± 5.8%) animals. Among positive neurons, CES and CCL had 'low to moderate' BDNF immunofluorescence in 60.5 ± 1.4% and 52.4 ± 3.5% of neurons respectively, greater than sham-ES (9.0 ± 2.8%) and unconditioned animals (19.1 ± 5.8%) ($p < 0.001$ for both). Interestingly, a significantly greater proportion of CES DRG neuronal cell bodies were 'highly' positive for BDNF (18.4 ± 2.3%) compared to those DRGs conditioned with CCL (9.4 ± 2.1%; $p < 0.05$). Both CES and CCL had a greater percentage of highly positive BDNF DRG neurons compared to the sham-ES and unconditioned animals (0.20 ± 0.1% and 0.04 ± 0.1% respectively). Western blot analysis confirmed increased expression of BDNF in CES and CCL ($p < 0.05$) compared to controls (Fig. 5F).

Increased expression of phosphorylated CREB (pCREB) was also observed among the conditioned cohorts (Fig. 5G-H). The percentage of CES DRG neurons with pCREB positively stained nuclei was 64.8 ± 0.7%, which was significantly higher than in the CCL group which had positive pCREB nuclear staining in only 42.8 ± 5.3% ($p < 0.05$). By contrast, sham-ES and unconditioned control animals had positive nuclear staining in 13.8 ± 0.7% and 9.7 ± 1.1% of cells, respectively, significantly less than CES ($p < 0.001$) or CCL ($p < 0.001$) (Fig. 5H). Western blot analysis confirmed both CES and CCL had significantly higher pCREB levels compared to sham-ES animals ($p < 0.05$ for both, Fig. 5I).

To investigate the response of the perineuronal SGCs to conditioning, GFAP upregulation was evaluated (Fig. 5J-K). CES yielded nearly identical upregulation of perineuronal SGC GFAP expression (52.8 ± 6.1%) compared to the traditional CCL (52.9 ± 6.4%) and were significantly higher than in the sham-ES (3.4 ± 2.1%) or unconditioned (2.1 ± 1.4%) control animals ($p < 0.001$ for both) (Fig. 5K). Western blot analysis confirmed both CES and CCL had significantly higher GFAP levels compared to sham-ES animals ($p < 0.05$ for both, Fig. 5L).

Together, these results suggest there is a comparable rise in the expression of RAGs in CES and CCL animals, suggesting similar conditioning paradigms were instigated. These results, however, do not explain the differences in sensory and motor outcomes between CES and CCL animals.

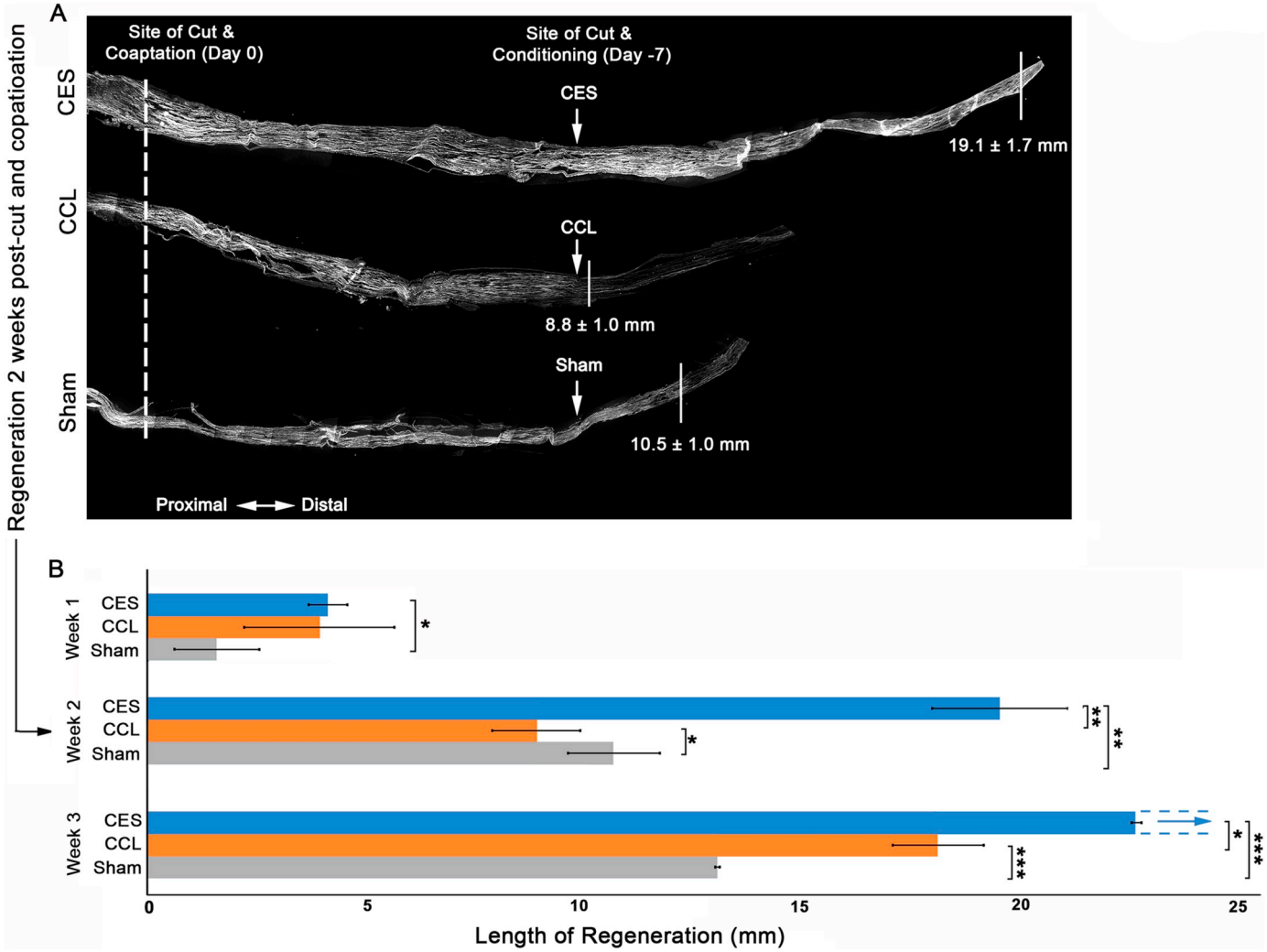

Fig. 6. Traumatic conditioning (CCL) delays regeneration. Representative photomicrographs of NF200-labeled longitudinal tibial nerve sections demonstrate the length of nerve regeneration at 7, 14, and 21 days post-coaptation in CES, CCL, and sham-ES animals. The white dotted line demarcates the site of cut and surgical coaptation, and the solid white lines delineate the distal-most point of axon regeneration per conditioning. Arrows indicate the site of conditioning (day −7) located 10 mm distal to site of surgical coaptation (day 0). At day 5, CES and CCL have similar lengths regeneration, both significantly longer than sham-stimulation (*$p < 0.05$). At day 14, axonal extension in CCL is arrested at the site of crush conditioning, whereas CES axons that do not have a second injury site to surpass continue to extend significantly longer than CCL (**$p < 0.01$) or sham (*$p < 0.05$). By day 21, CCL axons have passed the conditioning site and are regenerating faster than sham-ES (***$p < 0.001$); however, these axons fail to catch up to CES axons which have regenerated the entire length of the 2.2 cm tibial length harvested. Thus CES regenerated farther than CCL (*$p < 0.05$) and sham-ES (***$p < 0.001$) at 21 days following microsurgical nerve repair.

3.5. Regeneration in CCL is arrested by the conditioning site

In a further effort to determine the mechanism underlying improved functional recovery in the CES animals despite similar length of regeneration at one week and comparable expression of RAGs, we hypothesized that the difference was attributable to the injurious nature of a crush lesion. In our model, the crush lesion was delivered distal to the future site of cut and coaptation, therefore the regenerating axons had to traverse two injury sites: the site of transection, and the site of the CCL. By contrast, CES does not overtly damage the nerve. We therefore theorized that improved functional and behavioral outcomes of the CES animals may be because regenerating axons need only cross a single injury site. To determine the discrepancy in reinnervation outcomes between CES, CCL and unconditioned controls, the length of axonal extension was measured after 5, 14, and 21 days of regeneration (Fig. 6). In keeping with our 7 day data (Fig. 1), 5 days CES and CCL had similar rates of regeneration (4.1 ± 0.4 mm and 3.9 ± 1.5 mm, respectively) which were significantly more than the sham-stimulation negative control (1.6 ± 0.1 mm; $p < 0.05$). However, at 14 days post-coaptation, the relationship between CES and CCL changed; CES axons extended significantly longer (19.1 ± 1.7 mm) than CCL (8.8 ± 1.0 mm; $p < 0.01$) or sham-ES (10.5 ± 1.0 mm; $p < 0.01$). At this timepoint, CCL-conditioned axons were arrested at the site of crush conditioning (10 mm distal to the cut/coaptation site). By 21 days post-coaptation, the length of regeneration of CCL again extended significantly longer (17.8 ± 1.0 mm) than sham-ES (12.8 ± 0.1 mm; $p < 0.001$); however, they remained significantly shorter than CES axons (22.2 ± 1.0 mm; $p < 0.05$). Notably, the CES axons extended beyond the distal tip of the 2.2 cm of harvested tibial nerve (Fig. 6).

4. Discussion

Despite numerous advances in surgical techniques for peripheral nerve surgery, patient outcomes have not improved in the past two decades; this is largely attributable to the slow innate rate of nerve regeneration. Improving patient outcomes requires identification of a method to accelerate this process. A large body of convincing evidence supports CCL as an effective means of enhancing nerve regeneration in

animal models. However, this form of conditioning poses technical challenges that render it clinically infeasible. Over the past forty years, efforts have been made to identify a non-invasive method of delivering a conditioning-like effect. Unfortunately, all strategies attempted to date including vibration, freezing, ethidium bromide, and nerve compression, have failed to achieve the same magnitude of regeneration obtained by traditional CCL (Bondoux-Jahan and Sebille, 1986; Dahlin and Kanje, 1992; Dahlin and Thambert, 1993; Hollis 2nd et al., 2015).

Herein we identify CES as a novel form of nerve conditioning that, without mechanically injuring the nerve, exceeds regenerative outcomes observed with CCL. This is the first conditioning strategy that has achieved regeneration and reinnervation outcomes that supersede 'gold-standard' crush conditioning. More important, however, is the clinical feasibility of this technique. While electrical stimulation (ES) is previously well-described as a postoperative technique for promoting peripheral nerve regeneration (Al Majed et al., 2000a; Al Majed et al., 2000b; Geremia et al., 2007; Gordon et al., 2010; Gordon et al., 2008); its use as a preoperative conditioning modality *in vivo* is novel. As a postoperative intervention, the capacity of ES to enhance motor and sensory outcomes is limited by its underlying mechanism of action. PES only enhances regeneration across the site of repair (staggered regeneration) after which the rate of regeneration returns to that of an unconditioned animal (Gordon et al., 2009). In contrast, traditional crush conditioning accelerates the rate of regeneration along the entire length of the distal stump by upregulating regeneration associated genes, and expediting transportation of cytoskeletal elements actin and tubulin from the cell body to the growth cone. The first study investigating the use of ES as a conditioning lesion reported improved neurite extension comparable to CCL when outgrowth was measured *in vitro* (Udina et al., 2008). In a proof of principle study, we recently demonstrated that CES of the fibular nerve upregulates RAGs and, in response to a nerve transection and coaptation (test lesion), increases axonal elongation *in vivo* (Senger et al., 2017). Translation to a human clinical trial, however, requires a thorough investigation of the motor and sensory reinnervation outcomes to determine if the enhanced regeneration observed in the preliminary fibular nerve study results in improvements in functional outcomes.

To this end, in our current study, we demonstrated that not only does CES improve regeneration following tibial nerve transection and microsurgical repair, it also improves functional outcomes beyond that achievable with gold-standard CCL.

4.1. CES promotes nerve regeneration

Studies by Franz et al. (2008) demonstrated that the effects of electrical stimulation are variable in different nerves (Franz et al., 2008); therefore, we sought to compare the effects of CES on the tibial nerve with our previous observations in the fibular nerve (8). Although the total length of regeneration was greater following CES of the tibial (> 6.0 mm) compared to the fibular nerve (4.2 mm), so too was the innate regenerative capacity of their unconditioned controls (~2.7 mm, tibial; ~1.1 mm, fibular nerve) (Fig. 1). Although the regenerative capacity of the tibial nerve seems to be greater than the fibular nerve, the net benefits of conditioning, when normalized to their controls was 3.8-fold in the fibular nerve compared to ~2.5 fold in the tibial nerve. Taken together, these data suggest that the benefits of conditioning may be greater for nerves with a lower innate regenerative capacity. Despite differences in the length of regeneration, the number of axons crossing the coaptation site in CES (~120 axons) for both tibial and fibular nerves was greater than that of controls (~50 axons). This observation suggests that the inherent differences between the nerves are more likely to be attributable to the speed of regeneration rather than the magnitude of axonal sprouting. This observation is of significant clinical importance, as it suggests that CES may be of particular importance for patients with injuries to nerves with a poor innate regenerative capacity, such as the ulnar nerve (He et al., 2014).

4.2. CES promotes sensory and motor reinnervation

This is the first report of a minimally invasive conditioning intervention that meaningfully enhances sensory and motor functional outcomes compared to traditional crush conditioning. Our results suggest that CES significantly improves sensory reinnervation compared to both negative controls and CCL animals at 7–8 weeks (Figs. 2). Animals conditioned with ES had increased sensitivity to mechanical force which was supported by significantly higher IENF density counts in footpad biopsy specimens compared to CCL animals. Similarly, CES improved motor reinnervation outcomes beyond CCL animals, as indicated by toe-spread and foot placement analyses (Fig. 3), muscle mass recovery of the gastrocnemius muscle, and NMJ reinnervation (Fig. 4). These behaviour tests were confirmed electrophysiologically, with nerve conduction studies revealing significantly greater CMAP amplitude in the CES cohort.

These considerable improvements in sensorimotor functional outcomes are seemingly discordant with regenerative outcomes at one week, which demonstrates similar lengths of nerve regeneration in the CES and CCL cohorts. Unlike the noninjurious CES, however, CCL regenerating axons must cross two injury sites, the test lesion and the distal conditioning lesion site, which delays reinnervation. Despite similarities in length of axonal extension at 5 and 7 days, when CCL axons reached the site of conditioning 10 mm distal to the site of nerve coaptation, at 14 days post-repair, the speed of axonal extension in the CCL cohort was delayed whereas CES axons continued to extend. This delay to accommodate staggered regeneration in the CCL animals was so significant, that sham-ES axons caught up (Fig. 6). By 21 days of regeneration, axons in the CCL cohort surpassed the second (conditioning) site of injury, and extended beyond unconditioned nerves, but did not extend as far as the CES nerves. As such, axons in the CES cohort reached the distal end-targets first, allowing for earlier sensory and motor reinnervation. The similar pattern of RAG upregulation in both CES and CCL animals (in both tibial and fibular nerves) supports our findings of comparable growth rates (Fig. 5) (Senger et al., 2017).

4.3. Potential mechanisms responsible for the conditioning effects

As CCL evokes a significant immune response, inflammation has been credited, at least in part, to activate the pathways responsible for RAG upregulation (Kwon et al., 2013; Kwon et al., 2015; Sjoberg and Kanje, 1990). However, inflammation following CES is likely substantially less and thus its role in nerve regeneration in this paradigm is unclear. Typically, GAP-43 has been characterized as a 'nerve injury marker', GFAP as a 'glial cell injury marker', whereas BDNF and pCREB have been categorized as 'pro-regenerative markers' induced by nerve injury. Our findings suggest that nerve injury is not the only paradigm that regulates their expression. A potential mechanism for this that has gained increasing prominence is chromatin accessibility. In the CNS, this has been shown to play an important role in neuronal activity induced gene expression in dentate gyrus neurons (Su et al., 2017). Increased chromatin accessibility was also thought to result in enhanced regeneration of retinal neurons in young mice (Jorstad et al., 2017). Similarly, in the peripheral nervous system, chromatin regulators were found to be capable of altering the expression of a large set of RAGs following conditioning lesion (Loh et al., 2017). Together, these findings suggest that chromatin accessibility as a potent epigenetic mechanism is worthy of further exploration. Further studies investigating the common and divergent intracellular signaling cascades activated by CES and CCL, and potentially the resultant gene expression changes by unique chromatin regulation may elucidate their underlying mechanisms to promote nerve regeneration.

4.4. CES as a potential therapy

The importance of these findings lies in the direct translatability of

CES to the bedside. Since postoperative ES has already been shown to be safe and well-tolerated by patients (Gordon et al., 2010; Wong et al., 2015), preoperative delivery of electrical stimulation (ie: CES) would be acceptable to clinicians and patients alike. There are at least three clinical paradigms in which CES could be applied to improved patient outcome: (1) distal nerve transfers, (2) chronic nerve repair surgery (3) targeted muscle reinnervation for myoelectric prosthesis control.

In distal nerve transfers surgery, a “donor” nerve branch to a redundant muscle is transected and coapted to the distal end of a non-functional “recipient” nerve. The classic example is an Oberlin's transfer, in which the ulnar nerve branch to the flexor carpi ulnaris (FCU) muscle is transected and coapted to the distal stump of the musculocutaneous nerve branch to biceps brachii, in order to restore elbow flexion. Because flexor carpi radialis alone can flex the wrist, FCU is a ‘redundant’ muscle and loss of innervation has no functional effects. Similar transfers have been described to treat numerous nerve injuries in the upper and lower extremities. Nerve transfer surgery is elective, therefore the time of the transection of the donor nerve is scheduled; as such, patients could undergo percutaneous CES to the donor nerve in clinic 1 week prior to surgery, priming it for regeneration to enhance reinnervation of the target muscle.

Peripheral nerve injury is particularly common following major polytrauma necessitating emergent management of life or limb threatening injuries. In these situations, nerve injuries are often overlooked on initial exam, resulting in delays in repair beyond the suggested timeframe of three to 6 months post-injury (Jonsson et al., 2013). CES may be used as a tool to restore the regenerative capacity in these chronically denervated nerves. Furthermore, since postoperative ES is known to have different effects from CES, in that it reduces the delay caused by staggered regeneration without changing the speed of axonal outgrowth (Brushart et al., 2002), an interesting future option is to examine whether there is a synergistic effect when combining the two treatment modalities.

Targeted muscle reinnervation is a novel technique for improving the motor function of amputees. This surgery includes the transfer of viable nerves of an amputated limb into specifically selected muscles allowing EMG-induced signals to provide voluntary ‘spontaneous’ movements of a prosthesis. CES prior to nerve transfer may enhance NMJ reinnervation, and therefore the overall function of the prosthetic device.

CES is a noninjurious, clinically feasible method of enhancing nerve regeneration and sensorimotor functional recovery. This study presents comprehensive evidence that CES upregulates RAGs and enhances axonal growth similar to a CCL. We further reveal CES induces sensory and motor reinnervation and behavioral outcomes that supersede those obtainable by gold-standard conditioning methods. The importance of these findings, however, lies in their direct clinical applicability to improve outcomes in numerous peripheral nerve surgical challenges, as electrical stimulation is already established as safe and well tolerated. The use of CES in these clinical situations merits thorough investigation with randomized control trials, as it will likely significantly improve patient outcomes.

Acknowledgements

We would like to thank Doug Zochodne for his help and advice throughout this project. JLS was supported by a Canadian Institute for Health Research (CIHR) Graduate Scholarship. Grants from the CIHR, University Hospital Foundation (UHF) and the Edmonton Civic Employees Charitable Fund (ECE) helped fund this project (CAW and KMC).

Author contributions

JLS, AC and HM performed all experiments except the nerve conduction studies which were performed by KMC and KEJ. CAW, KMC and VMKV were involved with the experimental planning and design. CAW and JLS co-wrote the manuscript.

Potential conflicts of interest

We have no conflicts of interest to declare.

References

Al Majed, A.A., Brushart, T.M., Gordon, T., 2000a. Electrical stimulation accelerates and increases expression of BDNF and trkB mRNA in regenerating rat femoral motoneurons. Eur. J. Neurosci. 12, 4381–4390.
Al Majed, A.A., Neumann, C.M., Brushart, T.M., Gordon, T., 2000b. Brief electrical stimulation promotes the speed and accuracy of motor axonal regeneration. J. Neurosci. 20, 2602–2608.
Barber, B., Seikaly, H., Chan, K.M., Beaudry, R., Rychlik, S., Olson, J., Curran, M., Dziegielewski, P., Biron, V., Harris, J., McNeely, M., O'Connell, D., 2018. Intraoperative brief electrical stimulation of the spinal accessory nerve (BEST SPIN) for prevention of shoulder dysfunction after oncologic neck dissection: a double-blinded, randomized controlled trial. J. Otolaryngol. Head Neck Surg. 47, 4–13.
Bisby, M.A., 1985. Enhancement of the conditioning lesion effect in rat sciatic motor axons after superimposition of conditioning and test lesions. Exp. Neurol. 90, 385–394.
Bondoux-Jahan, M., Sebille, A., 1986. Electrophysiological study of conditioning lesion effect on rat sciatic nerve regeneration following either prior section or freeze. I. Intensity and time course. Brain Res. 382, 39–45.
Brushart, T.M., Hoffman, P.N., Royall, R.M., Murinson, B.B., Witzel, C., Gordon, T., 2002. Electrical stimulation promotes motoneuron regeneration without increasing its speed or conditioning the neuron. J. Neurosci. 22, 6631–6638.
Dahlin, L.B., Kanje, M., 1992. Conditioning effect induced by chronic nerve compression. An experimental study of the sciatic and tibial nerves of rats. Scand. J. Plast. Reconstr. Surg. Hand Surg. 26, 37–41.
Dahlin, L.B., Thambert, C., 1993. Acute nerve compression at low pressures has a conditioning lesion effect on rat sciatic nerves. Acta Orthop. Scand. 64, 479–481.
Franz, C.K., Rutishauser, U., Rafuse, V.F., 2008. Intrinsic neuronal properties control selective targeting of regenerating motoneurons. Brain 131, 1492–1505.
Geremia, N.M., Gordon, T., Brushart, T.M., Al Majed, A.A., Verge, V.M.K., 2007. Electrical stimulation promotes sensory neuron regeneration and growth-associated gene expression. Exp. Neurol. 205, 347–359.
Gordon, T., Brushart, T.M., Chan, K.M., 2008. Augmenting nerve regeneration with electrical stimulation. Neurol. Res. 30, 1012–1022.
Gordon, T., Chan, K.M., Sulaiman, O.A., Udina, E., Amirjani, N., Brushart, T.M., 2009. Accelerating axon growth to overcome limitations in functional recovery after peripheral nerve injury. Neurosurgery 65 (Suppl. 4), 132–144.
Gordon, T., Amirjani, N., Edwards, D.C., Chan, K.M., 2010. Brief post-surgical electrical stimulation accelerates axon regeneration and muscle reinnervation without affecting the functional measures in carpal tunnel syndrome patients. Exp. Neurol. 223, 192–202.
He, B., Zhu, Z., Zhu, Q., Zhou, X., Zheng, C., Li, P., Zhu, S., Liu, X., Zhu, J., 2014. Factors predicting sensory and motor recovery after the repair of upper limb peripheral nerve injuries. Neural Regen. Res. 9, 661–672.
Hoffman, P.N., 2010. A conditioning lesion induces changes in gene expression and axonal transport that enhance regeneration by increasing the intrinsic growth state of axons. Exp. Neurol. 223, 11–18.
Hollis 2nd, E.R., Ishiko, N., Tolentino, K., Doherty, E., Rodriguez, M.J., Calcutt, N.A., Zou, Y., 2015. A novel and robust conditioning lesion induced by ethidium bromide. Exp. Neurol. 265, 30–39.
Jonsson, S., Wiberg, R., McGrath, A.M., Novikov, L.N., Wiberg, M., Novikova, L.N., Kingham, P.J., 2013. Effect of delayed peripheral nerve repair on nerve regeneration, Schwann cell function and target muscle recovery. PLoS One 8, e56484.
Jorstad, N.L., Wilken, M.S., Grimes, W.N., Wohl, S.G., VandenBosch, L.S., Yoshimatsu, T., Wong, R.O., Rieke, F., Reh, T.A., 2017. Stimulation of functional neuronal regeneration from Muller glia in adult mice. Nature 548, 103–107.
Kwon, M.J., Kim, J., Shin, H., Jeong, S.R., Kang, Y.M., Choi, J.Y., Hwang, D.H., Kim, B.G., 2013. Contribution of macrophages to enhanced regenerative capacity of dorsal root ganglia sensory neurons by conditioning injury. J. Neurosci. 33, 15095–15108.
Kwon, M.J., Shin, H.Y., Cui, Y., Kim, H., Thi, A.H., Choi, J.Y., Kim, E.Y., Hwang, D.H., Kim, B.G., 2015. CCL2 mediates neuron-macrophage interactions to drive proregenerative macrophage activation following preconditioning injury. J. Neurosci. 35, 15934–15947.
Loh, Y.E., Koemeter-Cox, A., Finelli, M.J., Shen, L., Friedel, R.H., Zou, H., 2017. Comprehensive mapping of 5-hydroxymethylcytosine epigenetic dynamics in axon regeneration. Epigenetics 12, 77–92.
Lundborg, G., 2000. A 25-year perspective of peripheral nerve surgery: evolving neuroscientific concepts and clinical significance. J. Hand. Surg. [Am.] 25, 391–414.
Metz, G.A., Whishaw, I.Q., 2009. The ladder rung walking task: a scoring system and its practical application. J. Vis. Exp.(28).
Niemi, J.P., DeFrancesco-Lisowitz, A., Roldan-Hernandez, L., Lindborg, J.A., Mandell, D., Zigmond, R.E., 2013. A critical role for macrophages near axotomized neuronal cell bodies in stimulating nerve regeneration. J. Neurosci. 33, 16236–16248.
Niemi, J.P., DeFrancesco-Lisowitz, A., Cregg, J.M., Howarth, M., Zigmond, R.E., 2016. Overexpression of the monocyte chemokine CCL2 in dorsal root ganglion neurons causes a conditioning-like increase in neurite outgrowth and does so via a STAT3

dependent mechanism. Exp. Neurol. 275 (Pt 1), 25–37.
Richardson, P.M., Verge, V.M., 1987. Axonal regeneration in dorsal spinal roots is accelerated by peripheral axonal transection. Brain Res. 411, 406–408.
Richardson, P.M., Miao, T., Wu, D., Zhang, Y., Yeh, J., Bo, X., 2009. Responses of the nerve cell body to axotomy. Neurosurgery 65, A74–A79.
Senger, J.L.B., Verge, V.M.K., Macandili, H.S.J., Olson, J.L., Chan, K.M., Webber, C.A., 2017. Electrical stimulation as a conditioning strategy for promoting and accelerating peripheral nerve regeneration. Exp. Neurol. 302, 75–84.
Sjoberg, J., Kanje, M., 1990. The initial period of peripheral nerve regeneration and the importance of the local environment for the conditioning lesion effect. Brain Res. 529, 79–84.
Su, Y., Shin, J., Zhong, C., Wang, S., Roychowdhury, P., Lim, J., Kim, D., Ming, G.L., Song, H., 2017. Neuronal activity modifies the chromatin accessibility landscape in the adult brain. Nat. Neurosci. 20, 476–483.
Torigoe, K., Hashimoto, K., Lundborg, G., 1999. A role of migratory Schwann cells in a conditioning effect of peripheral nerve regeneration. Exp. Neurol. 160, 99–108.
Udina, E., Furey, M., Busch, S., Silver, J., Gordon, T., Fouad, K., 2008. Electrical stimulation of intact peripheral sensory axons in rats promotes outgrowth of their central projections. Exp. Neurol. 210, 238–247.
Wong, J.N., Olson, J.L., Morhart, M.J., Chan, K.M., 2015. Electrical stimulation enhances sensory recovery: a randomized controlled trial. Ann. Neurol. 77, 996–1006.
Ying, Z., Misra, V., Verge, V.M., 2014. Sensing nerve injury at the axonal ER: activated Luman/CREB3 serves as a novel axonally synthesized retrograde regeneration signal. Proc. Natl. Acad. Sci. U. S. A. 111, 16142–16147.